

Experimental optimization of a nitrogen laser

A. VÁZQUEZ MARTÍNEZ AND V. ABOITES

*Laser Laboratory, Centro de Investigaciones en Óptica
Apartado postal 948, 37000 León, Gto., México*

Recibido el 24 de junio de 1992; aceptado el 10 de marzo de 1993

ABSTRACT. A low pressure Blumlein type nitrogen laser was designed and the main factors affecting its performance were experimentally optimized in order to improve its efficiency. These factors were: the gas conditions (flow and pressure), the charging voltage, the electrode profiles, the inter-electrode spacing, the capacitance relation C_1/C_2 of the two capacitors involved in the Blumlein configuration, and the characteristics of the spark gap (inductance, geometry and position). As a result of these studies, a good efficiency ($\epsilon = 0.8\%$) nitrogen laser was obtained, which compares favorably to other lasers reported.

RESUMEN. Se presenta el diseño de un láser de nitrógeno tipo Blumlein de baja presión. El láser presenta alta eficiencia (0.8%) gracias a la optimización de la geometría de la cámara de descarga y a la incorporación de un *spark gap* de baja inductancia ($L < 10$ nH). Se logra operación estable del láser para voltajes en el rango de 8 a 14 kV, presiones del gas entre 70 y 250 Torr, y frecuencias limitadas a 20 Hz. El láser proporciona pulsos de buena calidad con energías mayores a 5 mJ y anchos temporales menores a 4 ns.

PACS: 42.55.Em

1. INTRODUCTION

Nitrogen lasers are important because they can provide high-power short-duration pulses of ultraviolet radiation ($\lambda = 337.1$ nm). These lasers are widely used in pumping dye lasers, spectroscopy and fluorescence studies, fast speed photography, etc. [1]. The main advantage of nitrogen lasers is that they are cheap and easy to build. However, their efficiencies are very low (generally lower than 1%), which limits their applications. Thus, although they are supposed to be well known devices, theoretical and experimental research on them continue in order to obtain more efficient configurations.

Basically, there are two excitation schemes employed for pumping nitrogen lasers, the Blumlein circuit and the charge transfer circuit (see Fig. 1). Some people consider two more schemes, the so called "travelling wave" technique of excitation and the Polloni configuration; however, the first is based on the Blumlein circuit, and the second is a modified version of the charge transfer circuit.

The characteristics of the Blumlein and the charge transfer circuits have been compared by Fitzsimmons *et al.* in Ref. [2]. The authors have shown that the Blumlein scheme can provide higher efficiencies than the charge transfer one. This result has been confirmed by other works: Godard reports a laser based on the "travelling wave" scheme, which provided an efficiency of about 1% [3]. The efficiencies obtained from lasers employing the traditional Blumlein configuration [4, 5] are of about 0.2%. On the other hand, the

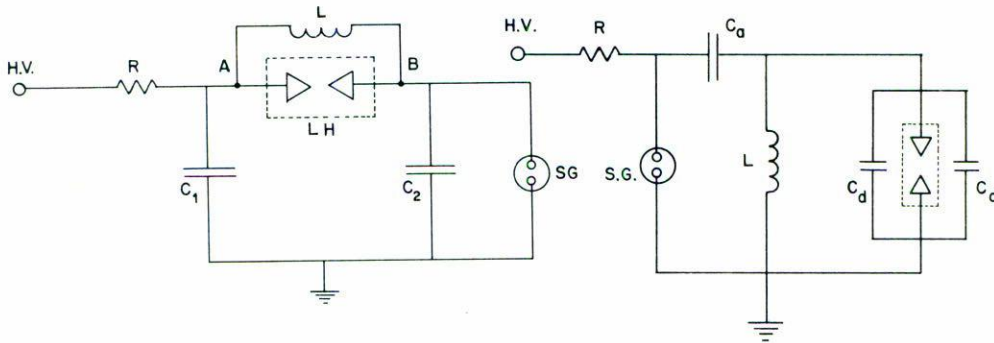


FIGURE 1. The two different circuits employed for pumping nitrogen lasers. a) Blumlein circuit. b) Charge transfer circuit. LH-laser head; SG-spark gap; L-coil; R-resistance; C_1 , C_2 -capacitors.

efficiencies obtained with the charge transfer scheme do not exceed 0.11% [6, 7]. However, there is a surprising exception to Fitzsimmons's result: Oliveira *et al.* reported a 3% efficiency nitrogen laser based on a Polloni configuration [8], which is very similar to a charge transfer scheme, except for a cylindrical capacitor involving the discharge chamber.

To our knowledge, except for Oliveira's report, there are not any other reports of efficiencies greater than 1%, even for nitrogen lasers of the same type [9, 10]. Thus, in the present work a Blumlein scheme was chosen, a laser was designed, and several experiments were carried out in order to find its best working conditions. We studied the dependence of the laser energy on the following parameters: 1) gas flow and pressure, 2) electrodes shape, 3) interelectrode spacing, 4) capacitance relation C_1/C_2 and 5) spark gap's geometry and inductance. The experiments allowed us to optimize the initial design and a high efficiency nitrogen laser was obtained, which can be useful in different applications.

2. THEORY

The schematic diagram of the Blumlein circuit is shown in Fig. 1a. It consists of two plane capacitors C_1 and C_2 parallel connected through the coil L . In the diagram, LH represents the laser head or discharge chamber and SG indicates the spark gap. The discharge across the laser head is achieved by abruptly discharging capacitor C_2 leaving C_1 charged; in this way a high voltage difference appears between the electrodes and the capacitor C_1 tends to discharge across the laser head.

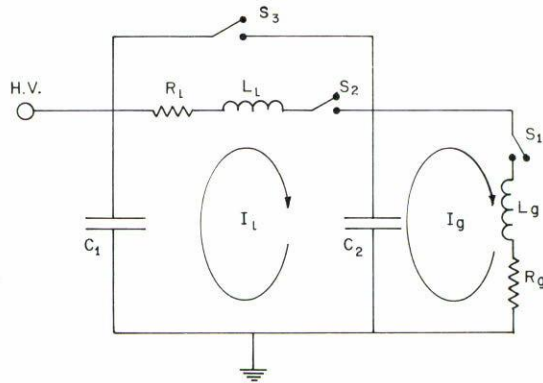


FIGURE 2. Equivalent circuit for the analysis of the Blumlein circuit.

A more detailed explanation of the performance of the Blumlein circuit can be as follows: Starting from zero volts, both capacitors are gradually and simultaneously charged at the same voltage and polarity. The full voltage difference appears across the spark gap while at the same time the voltage across the discharge chamber is zero. When the voltage across the spark gap reaches its breakdown value (let's say V_0), the spark gap triggers initiating the discharge of capacitor C_2 through it. Capacitor C_1 is not discharged at this stage because the discharge process is so fast that the impedance of the coil increases impeding any flux of current through it. Then, as capacitor C_2 discharges, the voltage in point B in Fig. 1a decreases and therefore the voltage difference across the laser head increases. Since this is a doubling circuit, this voltage difference is supposed to rise from zero toward a maximum value of about $2V_0$. However, the gas in the discharge chamber generally breaks at voltages lower than $2V_0$ and the voltage across the laser head will never reach this value unless the gas breakdown is purposely avoided (by increasing its pressure for example).

For theoretical analysis purposes, each discharge taking place in the circuit is simulated by an inductance and a resistance connected in series. The resultant equivalent circuit is shown in Fig. 2; in the diagram, R_1 and L_1 stand for the resistance and inductance associated with the discharge chamber, while R_g and L_g stand for the similar parameters associated with the spark gap. S_1 and S_2 are additional switches to indicate the onset of the discharges, and S_3 plays the role of the coil L .

Referring to Fig. 2, before the spark gap breaks down, the switch S_3 is closed, while S_1 and S_2 remain open. From the moment the spark gap breaks (S_1 closes) and before the main discharge takes place (before S_2 closes), there is a current I_g through the RLC circuit composed of R_g , L_g and C_2 . Since S_3 (the coil) opens at this stage, the voltage V_B in point B begins to drop, while the voltage V_A in point A remains constant. When the voltage difference $V_B - V_A$, *i.e.*, the voltage across the laser head, reaches a threshold value, the gas in the discharge chamber breaks down (S_2 closes) and a current I_1 flows through this second loop.

Thus, after the main discharge initiates, there are two simultaneous currents flowing through the circuit. These currents satisfy the following system of equations:

$$\begin{aligned} [L_g D^2 + R_g D + (1/C_2)]I_g - (1/C_2)I_1 &= 0, \\ [L_1 D^2 + R_1 D + (1/C_2) + (1/C_1)]I_1 - (1/C_2)I_g &= 0, \end{aligned}$$

where $D = d/dt$. Based on the experimental fact that the current and voltage recordings show an oscillatory behavior, oscillatory solutions can be proposed and the system of equations can be solved. An approximate solution to this problem is presented in Ref. [11].

For the purposes of the present work, we are only interested in the behavior of the circuit before the main discharge takes place because that will provide us with a method to calculate the inductance of the spark gap. If the main discharge is purposely avoided (by increasing the filling pressure for example), the voltage waveform $V(t)$ appearing across the capacitor C_2 is the voltage across the capacitor of the RLC circuit composed of R_g , L_g and C_2 itself. An example of such measurements is shown in Fig. 3; these voltage waveforms were recorded by using a high voltage probe and a wide bandwidth oscilloscope which are described in Sect. 4. By fitting the experimental curve to a damped oscillation of the form

$$V(t) = V_0 \exp(-t/\tau) \cos(\omega t),$$

the damping time constant τ and the angular frequency ω can be determined. Then the inductance L_g can be calculated from

$$\omega \cong (L_g C_2)^{-1/2}$$

and the resistance R_g from

$$\frac{1}{\tau} \cong \frac{R_g}{2L_g}.$$

This procedure was used to determine the spark gap inductance from the experimental measurements like the one shown in Fig. 3, the calculations are reported in Sect. 5.

3. EXPERIMENTAL

3.1. Laser construction

A laser based on a Blumlein configuration is very simple to build, which is important if we are going to optimize a given design. The laser built was especially designed to allow for easy modifications of its various components in order to find the optimal working conditions. For example, the capacitance values of the two capacitors could be varied by etching off copper material; the electrodes in the discharge chamber could easily be

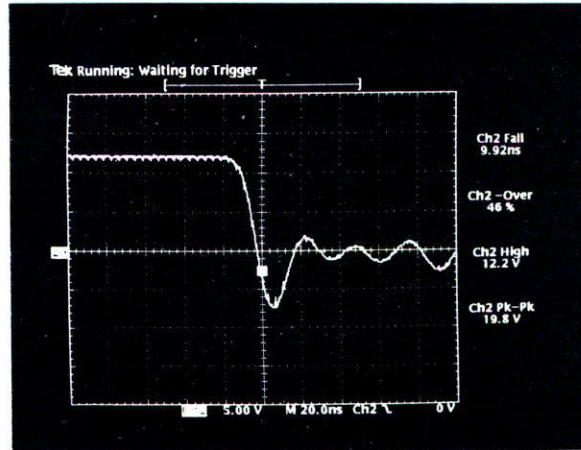


FIGURE 3. Voltage waveform appearing across capacitor C_2 when breakdown in the laser head is avoided. The characteristics of the waveform are automatically given by the oscilloscope (right upper corner). Horizontal scale-20 ns/div.

replaced by other electrodes of a different profile or material; the interelectrode spacing could be varied from 2 to 12 mm; the spark gap position could also be changed, etc.

The geometry of the laser is shown in Fig. 4. Basically, it consists of the discharge chamber, the capacitors and the spark gap. The capacitors were made from a double-sided copper circuit board with dimensions of $44 \times 64 \text{ cm}^2$ (1.5 mm thick). Copper material was etched from convenient places in order to make two equal capacitors with a common plate. The total capacitance $C_T = C_1 + C_2$ was 7.5 nF. The discharge chamber consists of two metallic pieces where 1 cm thick, 40 cm long electrodes can be inserted and fixed with screws. The discharge chamber is fixed to the board in good contact with the copper plates by using epoxy resin as shown in Fig. 5. The glass plate allows direct observation of the discharge, which is important for the detection of arcs or non-uniformities in it. There are quartz windows at Brewster angle at each end of the cavity. If no mirrors are used, there are equal outputs at each end; however, an aluminized mirror was placed at one end in order to obtain a single output.

Two different self-triggered spark gaps were tested, one externally connected to capacitor C_2 and other directly soldered on to it. Best results were obtained with the second one, whose geometry is shown in Fig. 6. It consists of two pieces which are soldered to the copper plates after opening a bore on the board. These two pieces are made of brass and they can house electrodes which can easily be removed. Its electrodes exhibit a spherical profile of 14 mm curvature. The separation between these electrodes can be varied from 0 to 10 mm, allowing the variation of the spark gap's breakdown voltage. In addition, this spark gap can be pressurized from 1 atm to 2 atm, which allows to reduce its inductance.

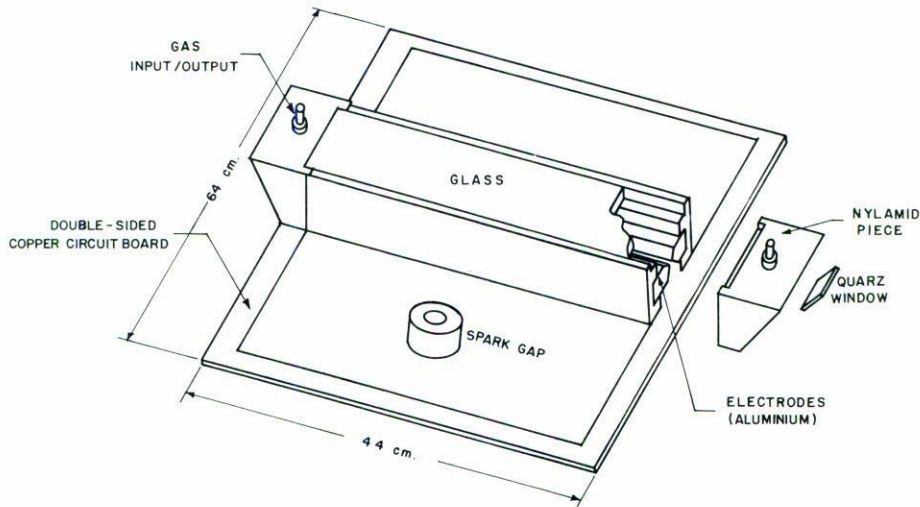


FIGURE 4. Schematic diagram of the laser built.

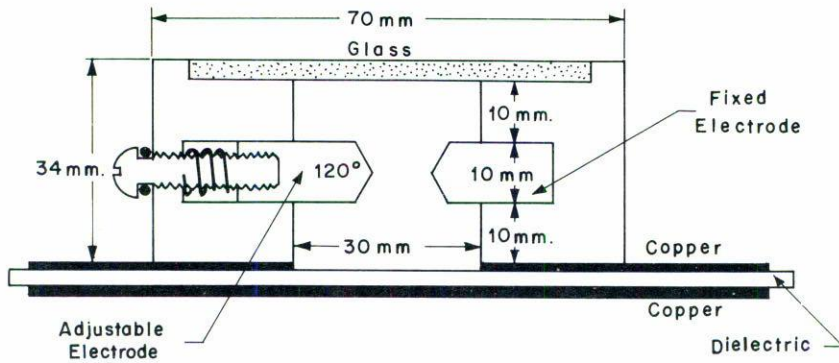


FIGURE 5. Detailed diagram of the discharge chamber.

3.2. Efficiency studies

Gas conditions. The dependence of the output laser energy on the gas pressure is well known. There is an optimal pressure value, for which energy is maximum. In the present work, we studied the laser energy as a function of pressure for different charging voltages. As can be seen from Fig. 7, the optimal pressure value is greater than 80 torr and it increases with the voltage. As for the gas flow, a continuous axial flow of pure nitrogen was established, at rates ranging from 3 to 15 lt/min. It was found that there is an optimal

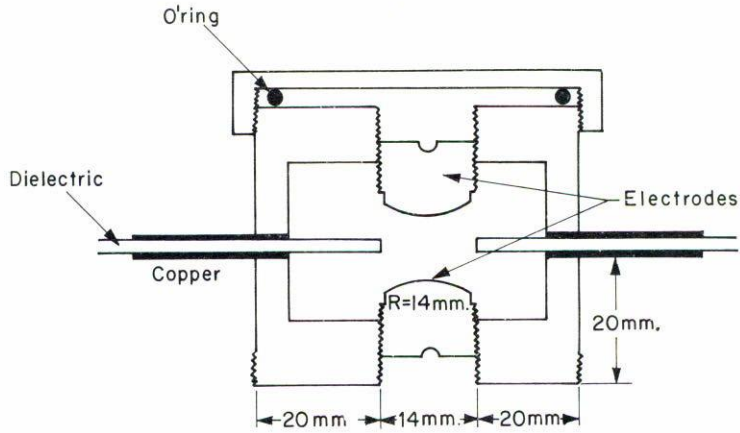


FIGURE 6. Detailed diagram of the spark gap.

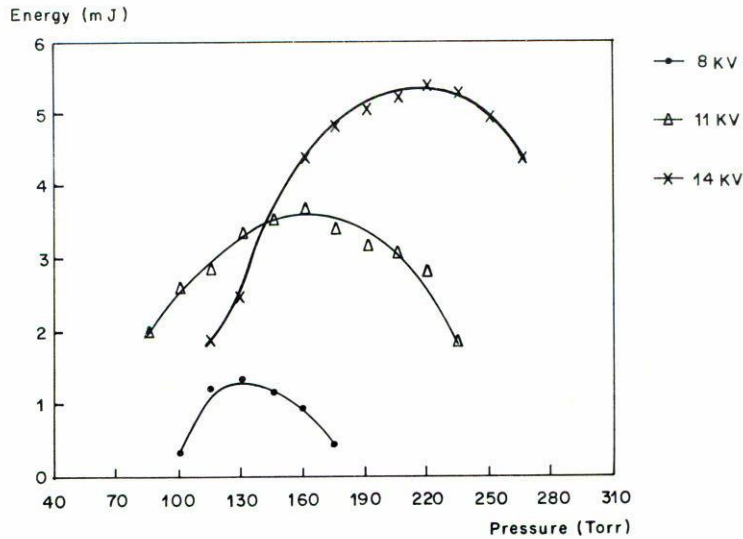







FIGURE 7. Laser energy as a function of gas pressure for different charging voltages.

rate of flow, which also depends on the particular working conditions: for higher charging voltages, higher flows were required.

Electrodes shape. In transversal gas discharge lasers, the shape of the electrodes is very important. The existence and stability of the main discharge depends to a great extent on this parameter. The problem of designing proper electrodes is serious even for small systems and several different configurations have been tested [12, 13]. In this work, three different types of electrodes were studied, flat electrodes, V-shaped electrodes and round-edged hexagonal ones. We tested equal electrodes and also combination of them; the results are summarized in Table I. As we can see, best results were obtained with

TABLE I. Different electrode configurations tested.

Electrodes profile	Observations
	No emission, a very weak glow discharge is produced.
	Low energy unstable pulses are observed, arcs are frequent due to border effects.
	No emission, no glow discharge, only arc discharges are present.
	No emission, a weak glow discharge is produced but arcs predominate.
	A very uniform and stable glow discharge takes place. Pulses with energies greater than 1 mJ are observed.

V-shaped electrodes. For this configuration, the discharge was very stable and uniform along the whole cavity.

Interelectrode separation. Another important parameter to be adjusted is the separation between the electrodes of the discharge chamber. This parameter determines the breakdown voltage and therefore affects the efficiency of the excitation. In the present work we studied the dependence of the laser energy on the interelectrode separation for the case of V-shaped electrodes. As can be seen from Fig. 8, the laser energy exhibits a strong dependence on this parameter. For the present design, the optimal separation turned out to be of about 8 mm.

Capacitance distribution. In Sect. 2 we saw that the Blumlein circuit employs two capacitors, which in general are made equal. The main role of capacitor C_2 is to form a doubling circuit in order to obtain a voltage difference of about $2V_0$ across the laser head. However, it was said that this voltage value is never reached because the gas generally breaks at lower voltages. Thus, one might think that the capacitor C_2 is somehow useless and that it could be eliminated or made smaller than C_1 . Then, there is the question of how to distribute the total capacitance C_T between the two capacitors in order to obtain the best laser efficiency. To answer this question, there is the recent work of Papadopoulos *et al.* (Ref. [11]), where they theoretically show that for the best laser efficiency both capacitors must be equal. In order to confirm this result in the laboratory, we carried out an experiment to study the dependence of the laser efficiency on the capacitance relation C_1/C_2 .

For the experiment, C_2 was kept constant whereas C_1 was varied by gradually etching copper from its upper plate. In Fig. 9, we show the laser efficiency as a function of the capacitance relation C_1/C_2 . The maximum efficiency was observed when capacitor C_1 was slightly greater than capacitor C_2 . From this result it is difficult to state a conclusion and further investigation is necessary. It seems to us that there is no a definite optimal distribution, but that depends on the particular circuit parameters (basically, the inductances

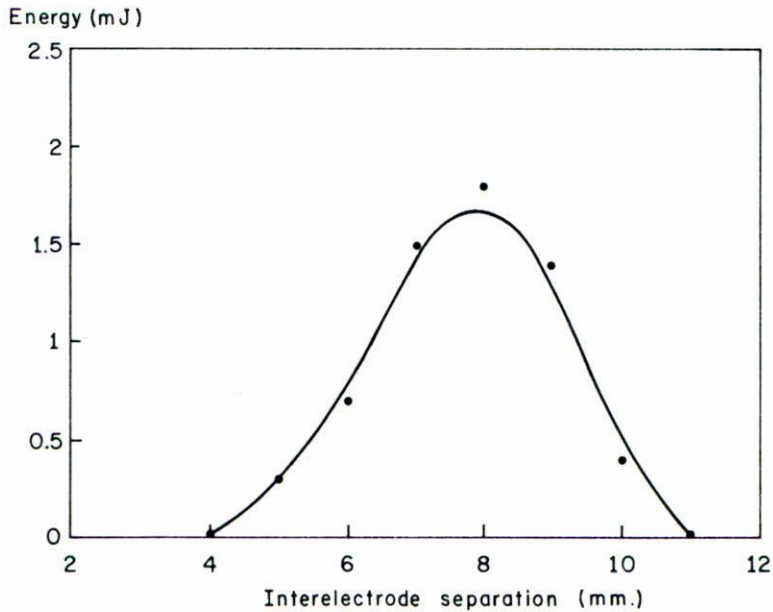


FIGURE 8. Laser energy as a function of interelectrode spacing for V-shaped electrodes.

and resistances associated with the discharge chamber and spark gap). It is important to note that according to the present results, the dependence of the efficiency on this relation is not very critical, especially for $(C_1/C_2) > 1$; for example, when the values of C_1/C_2 changes from 1 to 2, the variation on efficiency is only of about 20%. For $(C_1/C_2) < 1$, the variation of the laser efficiency becomes more important but not critical. In the final design, for the sake of simplicity, we decided to use the typical configuration with equal capacitors.

Spark gap operating conditions. The experimental work carried out in our laboratory showed that one of the most important factors affecting the laser efficiency was the spark gap performance. It was found that the operating conditions of the spark gap determined to a great extent the characteristics of the electrical pumping pulse, and therefore the pumping efficiency. This is so because in order to obtain good excitation of the upper laser level in nitrogen lasers, the temporal width of the pumping pulses must be as short as possible. Thus, special attention was paid to the spark gap and several different experiments were carried out to optimize its performance.

The most important parameter to improve on the spark gap is its inductance. In fact, it is well known that in a nitrogen laser not only the spark gap inductance must be minimized but all the inductances appearing in the system. As for the spark gap inductance, it basically depends on its geometry and dimensions. In the present work, we initially employed a traditional spark gap externally connected through wires to capacitor C_2 , but later changed to a new design of special geometry and small dimensions, which has been previously described in Sect. 3.1. Their inductances were calculated from experimental measurements as discussed in Sect. 2. For the first spark gap, its inductance turned out

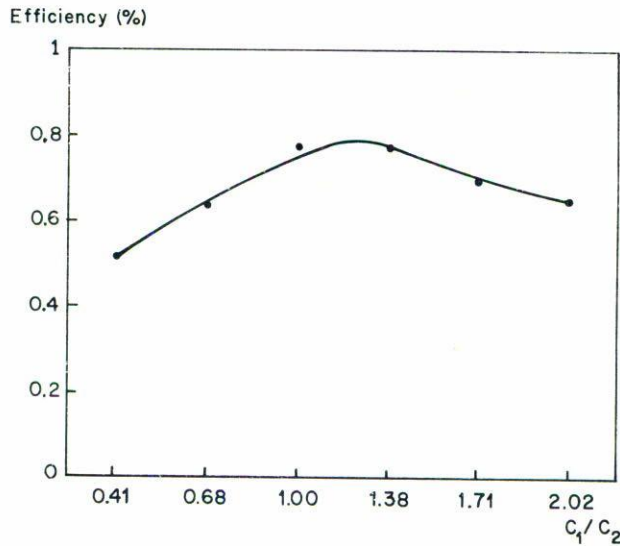


FIGURE 9. Laser efficiency as a function of the capacitance relation C_1/C_2 .

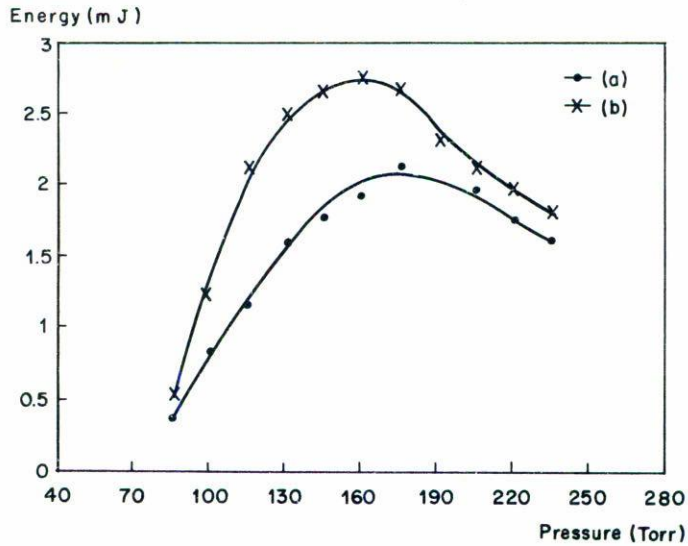


FIGURE 10. Energy as a function of pressure for two spark gaps with different inductances; (a) 70 nH, (b) 10 nH.

to be of about 70 nH ($R \cong 1.2 \Omega$), while for the second spark gap it was of about 10 nH ($R \cong 0.7 \Omega$). The effect of the spark gap inductance can be appreciated from Fig. 10, where a plot of the laser energy as a function of gas pressure is shown for the two different spark gaps. As it can be seen, the effect of this parameter on the laser efficiency is important, and it probably becomes more important for lower inductances (< 10 nH).

To optimize the spark gap we also studied the effect of the spark gap position, the

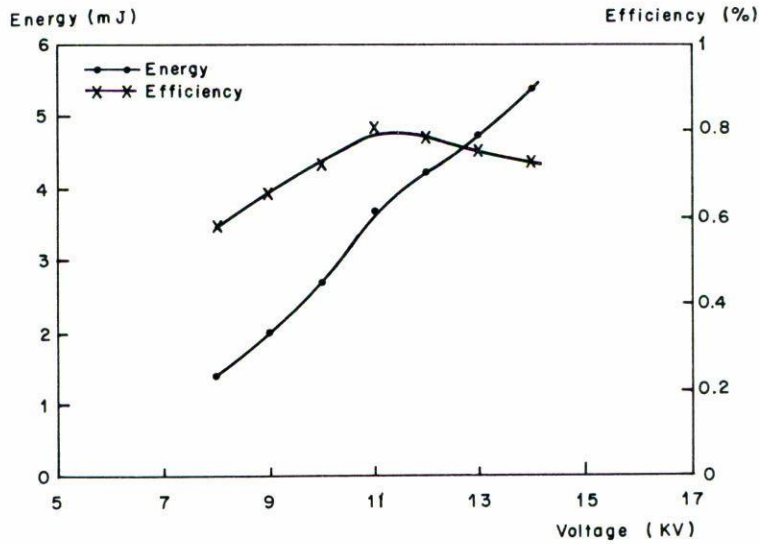


FIGURE 11. Maximum laser energy and efficiency as a function of voltage.

effect of the material of its electrodes and the effect of pressurizing it. We found that for better performance, the spark gap had to be placed at the center of capacitor C_2 . As for the material of its electrodes, we obtained better results with electrodes made of brass. When the spark gap was pressurized, its inductance diminished, leading to higher energies. Since this spark gap is self-triggered, the separation between its electrodes is also important because it affects its stability; stable operation of the spark gap was achieved for separations ranging from 2 to 5 mm (breakdown voltages between 7 and 12 kV).

4. RESULTS

In spite of the simplicity of the design, good results were obtained, especially in efficiency. The laser was made to operate at voltages ranging from 8 to 14 kV and the efficiencies observed were in the range of about 0.6% to 0.8%. The pulse repetition rate was limited to 20 pps; for higher rates the energy of the pulses showed a decrement. The charging voltage was kept below 15 kV because the spark gap triggering became irregular for higher voltages. The maximum observed energy was 5.4 mJ for a charging voltage of 14 kV (efficiency = 0.73%), while the maximum efficiency was 0.81% at 11 kV (energy = 3.7 mJ). These results are shown in Fig. 11, where the laser energy and efficiency are plotted as functions of the charging voltage.

The energy of the laser pulses was measured by using a pyroelectric Joulemeter (Molectron P3-01) and a Joulemeter Display (Molectron JD1000). The laser pulses were recorded with an MRD500 photodiode (risetime < 1 ns) together with a 500 MHz bandwidth oscilloscope (Tektronix TDS520). The voltage between the electrodes was measured by using two identical high voltage probes (Tektronix P6015, risetime < 4.5 ns). Two voltage probes

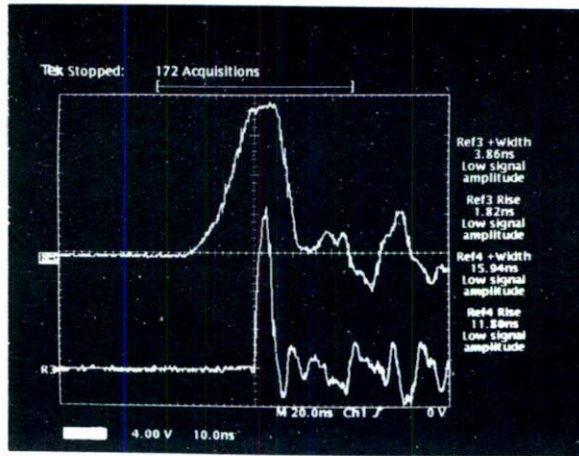


FIGURE 12. Simultaneous recording of the electrical and optical pulses. The electrical pulse is the one in the upper part. Horizontal scale-10 ns/div.

TABLE II. Comparison of the characteristics of the present laser with other previously reported lasers.

Reference	Laser type	E_{\max} [mJ]	Efficiency (%)
Schenk [13]	C-a-C	1.6	0.08
Godard [3]	Travelling wave		~1.0
Levatter [14]	Blumlein	20.0	0.12
Bergmann [5]	Blumlein-TEA	0.4	0.04
Iwasaki [4]	Blumlein-TEA	0.35	0.18
Armandillo [12]	C-a-C	25.0	0.10
Oliveira [8]	Polloni	3.0	3.0
Stankov [15]	C-a-C	1.0	0.03
Serafetinides [6]	C-a-C	12.0	0.11
Pinto [9]	Polloni	0.5	0.11
Papadopoulos [11]	Blumlein-TEA	2.9	0.15
Encinas [7]	C-a-C	20.5	0.02
Villagrán [10]	Polloni	1.2	0.38
<i>Present work</i>	Blumlein	5.4	0.81

were required because for the recording of this voltage waveform one needs to measure the voltage waveform in each electrode simultaneously and then obtain the voltage difference.

Figure 12 shows a simultaneous recording of both the optical and electrical pulses observed under optimal conditions. The characteristics of the pulses were automatically given by the oscilloscope. The width of the light pulses were typically less than 4 ns, while the width of the electrical pulses were less than 20 ns. The short duration of the electrical

pulse, attributed to the low inductance of the spark gap, guarantees an efficient excitation of the gas.

In order to show the importance of the present results, in Table II, the characteristics of the present design are presented, together with those of some other lasers reported. It can be seen that the present laser compares favorably to the lasers reported: it doesn't provide very high energy pulses but its efficiency is good.

5. CONCLUSIONS

A high efficiency Blumlein type nitrogen laser for voltages not exceeding 14 kV has been described. The high efficiency observed is a result of experimental studies, which allowed us to find the best working conditions for the laser. The design is simple both in construction and operation and a detailed description of it has been given. The characteristics of the laser pulses make them useful for various applications, in pumping a dye laser for example. At the moment, an improved version of this design is being developed in order to get higher energies.

REFERENCES

1. J.P. Singh and S.N. Thakur, *J. Sci. Ind. Res.* **39** (1980) 613.
2. W.A. Fitzsimmons, L.W. Anderson, C.E. Riedhauser, and J.M. Vrtilek, *IEEE J. Quantum Electron.* **QE-12** (1976) 624.
3. B. Godard, *IEEE J. Quantum Electron.* **QE-10** (1974) 147.
4. Ch. Iwasaki and Takahisa Jitsuno, *IEEE J. Quantum Electron.* **QE-18** (1982) 423.
5. E.E. Bergmann, *Appl. Phys. Lett.* **28** (1976) 84.
6. A.A. Serafetinides, *Opt. Comm.* **72** (1989) 219.
7. F. Encinas Sanz and J.M. Guerra Perez, *Appl. Phys. B* **52** (1991) 42.
8. B. Oliveira dos Santos, C.E. Fellows, J.B. de Oliveira e Souza, and C.A. Mason, *Appl. Phys. B* **41** (1986) 241.
9. V.J. Pinto and Vicente Aboites, *Inst. y Des.* **2** (1985) 341.
10. M. Villagrán, J. Garduño, J. de la Rosa, R. Linares, submitted for publication to *Inst. y Des.* (1991).
11. A.D. Papadopoulos and A.A. Serafetinides, *IEEE J. of Quantum Electron.* **QE-26** (1990) 177.
12. E. Armandillo, *Appl. Phys. Lett.* **41** (1982) 611.
13. P. Schenk and H. Metcalf, *Appl. Opt.* **12** (1973) 183.
14. J.I. Levatter and Shao-Shi Lin, in *Appl. Phys. Lett.* **41** (1974) 703.
15. K.A. Stankov, S.Z. Kurtev and I.Y. Milev, *Opt. Comm.* **62** (1987) 32.